2018

# Impacts of Climate Change on the State of Indiana: ensemble future projections based on statistical downscaling

Alan Hamlet
*University of Notre Dame*, hamlet1@nd.edu

Kyuhyun Byun
*University of Notre Dame*

Scott Robeson
*Indiana University*

Melissa Widhalm
*Purdue University*, mwidhalm@purdue.edu

Mike Baldwin
*Purdue University*

**Impacts of Climate Change on the State of Indiana: ensemble future projections based on statistical downscaling**

Alan F. Hamlet [1]

Kyuhyun Byun [1]

Scott Robeson [3]

Melissa Widhalm [4]

Michael Baldwin [2]

1 Corresponding Author, Department of Civil and Environmental Engineering and Earth Sciences, University of Notre Dame, 156 Fitzpatrick Hall, Notre Dame, IN 46556, hamlet.1@nd.edu, 574-631-7409

2 Department of Earth, Atmospheric, and Planetary Sciences, Purdue University

3 Department of Geography, Indiana University, Bloomington

4 Climate Change Research Center, Purdue University

Key Words:

Indiana, climate change impacts, CMIP5, hybrid delta, temperature and precipitation, length of growing season, hardiness zones, cooling degree days, heating degree days.

**Abstract**

Using an ensemble of 10 statistically downscaled global climate model (GCM) simulations, we project future climate change impacts on the state of Indiana (IN) for two scenarios of greenhouse-gas concentrations (a medium scenario--RCP4.5, and a high scenario--RCP 8.5) for three future time periods (2020s, 2050s, 2080s). Relative to a 1971-2000 baseline, the scenarios project substantial changes in temperature for IN, with a change in the annual ensemble mean temperature for the 2080s RCP8.5 scenario of about 5.6 °C (10.1 °F). Such changes also indicate major changes in extreme temperatures. For southern IN, the number of days with daily maximum temperatures above 35 °C (95 °F) is projected to be about 100 days per year for the 2080s RCP8.5 scenario, as opposed to an average of 5 days for the historical baseline climate. Locations in northern IN could experience 50 days per year above 35 °C (95 °F) for the same conditions. Energy demand for cooling, as measured by Cooling Degree Days (CDD), is projected to increase nearly fourfold in response to this extreme warming, but heating demand as measured by Heating Degree Days (HDD) is projected to decline by 30%, which would result in a net reduction in annual heating/cooling energy demand for consumers. The length of the growing season is projected to increase by about 30 to 50 days by the 2080s for the RCP8.5 scenario, and U.S. Department of Agriculture hardiness zones are projected to shift by about two half zones throughout IN. By the 2080s, all GCM simulations for the RCP8.5 scenario show higher annual precipitation (P) over IN. Projected seasonal changes in P include a 25-30% increase in winter and spring P by the 2080s for the RCP8.5 scenarios and a 1-7% decline in summer and fall P (although there is low model agreement in the latter two seasons). Rising temperatures are projected to result in systematic decreases in the snowfall-to-rain ratio from Nov-Mar. Snow is projected to become uncommon in southern IN by the 2080s for the RCP8.5

scenario, and snowfall is substantially reduced in other areas of the state. The combined effects of these changes in T, P, and snowfall will likely result in increased surface runoff and flooding during winter and spring.

## 1. Introduction

Regional studies of climate change (CC) are instructive because of the expected consistency of impacts over similar geographical areas. States in the Midwestern region of the U.S. are a case in point and they are frequently analyzed together as a homogeneous region (e.g. Winkler et al. 2012; Byun and Hamlet 2018). The Midwestern states, however, exhibit considerable variability in climate with both latitude and longitude. For example, the western and northern portions of the Midwest are considerably drier than the eastern and southern portions of the domain, and there are substantial increases in temperature from north to south.

In addition to better characterizing subregional heterogeneity, there is a need to provide CC information at scales that support local planning efforts and that facilitate meaningful engagement with diverse stakeholders whose interests are affected by climate. Urban planners in Minneapolis, Chicago, Indianapolis, and Cincinnati, for example, face similar kinds of problems related to CC that are affecting the Midwest as a whole (e.g., increases in extreme heat, humidity, and precipitation), but the design of sustainable and resilient infrastructure in the four cities requires detailed CC projections that reflect the distinct baseline conditions for each city and the local effects of CC. One useful way to subset a region such as the Midwest, therefore, is to focus on climate change impacts at multiple administrative units, such as states, counties, and cities.

In this study, we provide CC projections at a very fine spatial scale for the state of Indiana (IN) in the U.S. using statistically downscaled gridded data sets based on the Coupled Model Intercomparison Project, Phase 5 (CMIP5, Taylor et al. 2012) associated with the Intergovernmental Panel on Climate Change Fifth Assessment Report (IPCC AR5). This detailed statewide study supports the Indiana Climate Change Impacts Assessment (IN CCIA)

(http://www.purdue.edu/discoverypark/climate/in-ccia/), led by the Purdue Climate Change Research Center, in partnership with the University of Notre Dame, Indiana University, the Midwestern Regional Climate Center, and Ball State University.

## 2. Regional Climate Change Context

For the two most widely used greenhouse-gas scenarios, Representative Concentration Pathways (RCP) 4.5 and 8.5 (Moss et al. 2008) (representing "medium" and "high" 21$^{st}$ century greenhouse-gas concentration trajectories), the Midwestern U.S. is projected to experience profound changes in climate by 2100, especially for temperature. Projections for annual mean air temperature over the Midwestern U.S. from 31 Global Climate Models (GCMs) for the RCP8.5 scenario show an ensemble mean increase in T of about 6.5 °C (11.7 °F) by 2100 relative to the historical 1971-2000 baseline (Figure S1) (Byun and Hamlet 2018). The projected change in the annual ensemble mean for RCP4.5 over the Midwestern U.S. is about 3.3 °C (5.9 °F) by 2100 relative to the 1971-2000 baseline. The upper tail of the annual mean temperature distribution, represented by the 97.5$^{th}$ percentile of the 31 GCM projections for RCP8.5 (i.e. a "worst-case" scenario), is nearly 10 °C (18 °F) warmer than the historical baseline by 2100. The ensemble mean values are about 1.7 °C (3.1 °F) larger than the projected global average temperature increase over land reported by the IPCC (~4.8 °C (8.6 °F) by 2100 for RCP 8.5) (IPCC AR5 2013). As is apparent from Figure S1, the signal-to-noise ratio for air temperature is very large, so detecting temperature shifts of this magnitude over time will not be difficult or ambiguous from a statistical perspective (Byun and Hamlet 2018). For example, by the 2050s, the 2.5$^{th}$ percentile of the GCM simulations is already larger than the simulated 97.5$^{th}$ percentile for the mid-20$^{st}$ century climate. Consistent with results at the global scale (IPCC, 2013), meaningful

differences in annual air temperature between a “medium” (RCP 4.5) and “high” (RCP 8.5) emissions scenario are not evident until after the 2040s, suggesting that our collective ability to change temperature trajectories over the next 25 years may be minimal, even if concerted efforts are focused on reducing relatively short-lived greenhouse gasses such as methane or nitrous oxide (Smith and Mizrahi, 2013). Changes in summer temperatures show little spatial variability across the Midwestern U.S., whereas changes in winter temperature are largest in the northernmost and smallest in the southernmost parts of the domain (primarily due to snow-albedo and water-vapor feedbacks and differences in the relative importance of outgoing longwave radiation in winter) (Byun and Hamlet, 2018). As a result, the existing latitudinal gradient in winter-mean temperature over the Midwest is projected to become somewhat less pronounced over time.

Annual precipitation totals over the Midwest are projected to increase for all models by the 2080s for RCP 8.5, but the changes are most pronounced in winter (DJF) and spring (MAM) (Figure S2). Mean changes in summer (JJA) and fall (SON), by comparison, are relatively small and the direction of change during these seasons is not consistent across the different GCM simulations (Figure S2; Byun and Hamlet 2018). In other words, the signal-to-noise ratio for projected precipitation change is relatively high in winter and spring and relatively low in summer and fall. Even though these results are downscaled, it is worth noting that GCMs, because of their coarse spatial resolution, currently are not able to explicitly capture changes in small-scale convective storms., As a result, some caution should be exercised in interpreting warm-season precipitation statistics over IN, for which a substantial fraction of precipitation is associated with convective storms. This also implies that, in assessing changes in summer

precipitation, the use of dynamical downscaling using high-resolution regional climate models is preferred due to the ability of such models to explicitly simulate convective storms in a physically based manner (see e.g. Liu et al. 2016; Prein et al 2018). For similar reasons, we do not attempt to downscale coarse-resolution GCM-simulated wind speed in this study.

We also note that there are some important linkages between changes in P and T, particularly in summer. It has been commonly found in past studies, for example, that the driest GCM scenarios in summer tend to also have the largest increases in T (see e.g. Rupp et al. 2013). We show in the results section below that this is also the case for IN, but that there are additional connections between strong warming and wetter conditions that seem to be unique to the Midwest region.

## 3. Data and Methods

### *3.1 Statistically Downscaled CMIP5 Climate Projections*

A comprehensive assessment of CC impacts in Indiana requires an integrated approach using several different kinds of observed data sets and downscaling approaches. Historical baselines for this study are provided by 1/16$^{th}$ degree latitude-longitude (~5 x 7 km) gridded meteorological data sets from 1915-2013 prepared over the Great Lakes and Midwestern States (Chiu et al. in review). These historical data are corrected to account for precipitation gauge undercatch as a function of precipitation type (i.e., snow, mixed rain and snow, and rain) and wind speed. Statistical downscaling techniques used here are based on monthly GCM simulations and provide a range of expected results based on an ensemble of 10 GCM projections selected to capture the range of results from 31 different models (Byun and Hamlet 2018). As used here, statistical downscaling facilitates an informed sensitivity analysis of the

effects of changing climate on IN as a function of future greenhouse gas concentration (GGC) scenarios.

Dynamical downscaling using high-resolution regional-scale climate models can provide physically based simulations of impacts that may not be adequately captured by statistical downscaling (e.g., interarrival time of storms, extreme wind, extreme humidity, precipitation from summer convective storms, and lake-effect snow). Dynamical downscaling, however, because of its much greater computational requirements, is often is limited to the use of a single large-scale (global) forcing scenario, and therefore does not evaluate the range of GCM-derived uncertainty that statistical downscaling can more easily accommodate. In addition, after applying bias corrections based on observed probability distributions, statistical downscaling is particularly apt for evaluating projections of extreme temperature and precipitation at fine spatial scales (Schoof and Robeson 2016; Byun and Hamlet 2018). Thus the two downscaling approaches complement each other by addressing different needs. For the remainder of this paper, we focus solely on results from statistical downscaling.

Climate-change projections in this paper are evaluated using a suite of GCM simulations from the Coupled Model Intercomparison Project, Phase 5 (CMIP5; Taylor et al. 2012). Course-resolution GCM output is downscaled by the Hybrid Delta (HD) statistical downscaling approach (Tohver et al. 2014; Hamlet et al. 2013; Byun and Hamlet 2018) to 1/16$^{th}$ degree grid resolution (~5 x 7km). As the name suggests, the HD is a hybrid approach combining monthly shifts in the T and P probability distributions deriving from the well-known Bias Correction and Spatial Downscaling (BCSD) approach (Wood et al. 2002, 2004) with observed storm characteristics and accurate daily time series behavior (including extremes) deriving from gridded station observations. The HD approach produces a long time series of observed

variability (1915-2013 in our case), superimposed on systematic changes in monthly probability distributions deriving from GCM simulations of future climate. Thus the HD future projections have the same sample size and essentially the same time series behavior as the historical baseline. A specific year, month, or day from the future time series can be directly compared to its historical counterpart (e.g. water year 1933 from the historical baseline can be directly compared to its future counterpart water year "cc-1933"). These features of the HD make it very useful for calculating long-term climate statistics and estimating hydrometeorological extremes, because the historical and future products all have the same large sample size (99 years of daily data) and incorporate realistic storm and drought characteristics deriving from a long historical record. The strengths of the approach also imply some limitations, however, since the number of dry and wet days, the size and interarrival time of storms, and other contingent characteristics are inherited from the historical record and do not change in the future projections. Hamlet et al. (2013), Tohver et al. (2014), and Byun and Hamlet (2018) provide additional technical details on implementation and validation of the HD approach.

For each greenhouse gas scenario, an ensemble of 10 representative GCM projections from the CMIP5 archive have been statistically downscaled for the 2020s (2011-2040), 2050s (2041-2070), and 2080s (2071-2100) using the HD approach over the entire Midwest region (Byun and Hamlet 2018). Methods used in selecting the 10 representative GCMs from a larger ensemble of 31 GCMs are reported in more detail by Byun and Hamlet (2018), but we give a brief overview here to help orient the reader. Using 31 GCMs from the CMIP5 archive, changes in annual T and P were calculated over the Midwest for the RCP 8.5 emissions scenario for the 2080s. The performance of the models in reproducing observed climate in the Midwest was also evaluated, and the models were ranked according to their performance. Three groupings of

GCMs were then selected based on two separate criteria: a) model performance (top half of the performance ranking), and b) ability to capture, in the subsample, the range of changes in T and P from the full ensemble. The first grouping is a single model representing the central tendency of the entire 31-member ensemble. The second group adds five models from the outer perimeter of the delta T and P space (total of six ensemble members). The third group adds four additional members from an inner circle (total of 10 ensemble members) to flesh out the internal parts of the probability distribution (see Figure 5 from Byun and Hamlet 2018). Although the selection is made using annual changes in T and P, Figure S2 shows that the 10-member ensemble also captures the range and central tendency of the full 31-member ensemble for different seasons reasonably well. For the analyses that we show in this paper, unless otherwise noted, the full 10-member ensemble is used.

The end products produced by the HD downscaling method are gridded daily data sets at $1/16^{th}$ degree resolution that can be masked to produce summary results at a wide range of spatial scales including state- or county-wide averages, results for specific cities, or detailed state-wide maps. In addition to the summary results produced for this paper, these data have been provided to several other working groups participating in the INCCIA to support their analyses, as reported in the other papers that make up this special issue.

### 3.2 *Data Processing Methods for Summary Results*

The analyses presented in this paper are based on three types of basic data processing techniques, which are outlined in Table 1. We will use abbreviated descriptions in figure captions to identify the method used to produce each figure. For example, Figure 1 is a product

produced using Type III data processing, with data averaged in space over the entire domain (IN), and then presented as a composite mean plot.

## 4. Results and Discussion

This section is divided into three main subsections, the first focusing on T and P impacts, the second focusing on impacts to growing-season length and U.S. Department of Agriculture (USDA) hardiness zones, and the third on impacts to heating and cooling degree days.

### *4.1 Summary of Temperature and Precipitation Changes*

#### *4.1.1 Temperature Changes*

Similar to the rest of the Midwest, temperature-related impacts are expected to be substantial in Indiana (Figure 1) By mid-21$^{st}$ century, temperature changes are more pronounced in summer than in winter. March and November show systematically lower amounts of warming than other months, and by the 2050s the largest temperature changes are in August. As expected, temperature changes are systematically larger for RCP 8.5 than for RCP 4.5 and increase with time for each greenhouse-gas scenario (see also Figure S1).

Spatial patterns of warming are somewhat dependent on season, but in general there is little spatial variability over IN. Table 2A summarizes the change in T for each time period and emissions scenario. Note that the spatial standard deviation of changes in T is much smaller than the change in delta T for all seasons.

The annual number of frost days (days with Tmin < 0 °C (32°F)) in IN decreases steadily during the 21$^{st}$ century (Figure 2), although there are still a relatively large number of frost days in winter even for the most extreme warming scenario (2080s RCP8.5). Northern IN, for example, is projected to experience a 45% decrease in the number of frost days (from 135 per

year for the baseline), but still has about 75 frost days per year on average even for the 2080s RCP8.5 scenario.

The number of days with extreme hot temperatures (Tmax > 35°C (95°F)) in IN is projected to increase dramatically with warming (Figure 3). By the 2080s, the RCP8.5 scenario shows extreme changes in the frequency of very hot days, especially in southern IN. In Evansville (in the southwest corner of the state), for example, the ensemble average number of very hot days increases to about 100 days per year from about 10 for the historical baseline climate. Table S1 shows the baseline and future projections of the number of extreme hot days for selected urban areas in Indiana. In northern IN, the ensemble mean number of extreme hot days increases to about 60 days per year on average for the 2080s RCP8.5 scenario from a historical baseline of about 3 days per year.

Although these projections point unambiguously to important T impacts in the Midwest and IN, there are some important caveats to be made. To begin with, an examination of historical trends in annual average T (Figure S3) and the number of days with statewide average maximum T above 32.2 °C (90 ° F) (Figure S4) shows that natural climate variability in the 20$^{th}$ century (and particularly the megadroughts of the Dust Bowl years in the 1930s and 1940s) has played an important role in determining annual average and extreme high T regimes in IN. The extreme drought conditions during the Dust Bowl years, for example, resulted in approximately 35 days per year with daily maximum T above 32.2 ° C (90 °F). Since 1960, the average number of days above 32.2 ° C has decreased to about 15 days per year on average, with no significant trend since 1960 (Figure S4). One study (Mueller et al. 2016) has argued that increased evaporation due to changes in crops and increasing use of irrigation may have played a key role in the observed systematic shift in extreme summer temperatures, but this analysis excluded the

Dust Bowl years and also data prior to 1910. An alternate explanation is simply that T feedbacks from increased P have been observed starting in about 1960 after several decades of very dry conditions. This better explains the available data from 1895-1915 shown in Figure S3, for example, which show a similar average T regime to the post-1960 data, without the crop and evaporation changes identified by Mueller et al. (2016).

Although land use, irrigation, and vegetation changes are not explicitly included in this study, linkages between drought cycles and T are present in the climate change projections, especially in summer. Figure S5 shows the relationship between delta T and delta P for the ensemble of 10 summer projections for three time periods and two greenhouse gas concentration scenarios. The analysis identifies two dominant and opposing relationships between delta T and delta P: one showing unusually dry conditions associated with warmer conditions, and the other showing wetter conditions associated with warmer conditions. The first relationship is most pronounced and consistent across different periods and concentration scenarios. Our hypothesis is that the first regime is related to increased solar radiation (reduced cloudiness) and systematic increases in the Bowen ratio (ratio of sensible to latent heat flux) that accompany low water availability at the land surface.The second relationship is likely caused by increased advection of warm and humid air from the Gulf of Mexico or the Atlantic coast, resulting in relatively warm and wet conditions. These results show that extreme summer heat in the future could be caused either by unusually dry summer conditions or by increased warm, moist air being advected into the region. It's clear, however, that the largest increases in T in summer accompany the driest scenarios, especially for the RCP8.5 2080s. For example, a reduction in summer precipitation on the order of 30% results in extreme warming of about 10 °C in the projections, whereas scenarios with more modest reductions in P result in only about 5 °C

warming (Figure S5).

Taken together, analysis of historical trends and future projections in daily maximum T suggest that extreme heat scenarios in IN could prove to be highly variable in time and may be linked to relatively uncertain summer P impacts. The relatively weak model agreement on summer P changes (Byun and Hamlet 2018), for example, suggests that impacts to summer P (and therefore extreme high temperatures) may vary substantially from decade to decade in response to natural climate variability, despite overall increases in average T. In the most extreme case, a recurrence of extreme drought conditions like those experienced in the 1930s and 1940s could result in unprecedented, catastrophic heat impacts when coupled with the strong systematic warming in the future projections. Although this would appear to be a worst-case scenario, such extreme changes in P and T cannot be ruled out and could emerge without warning in just a few years' time and then persist for several decades, as occurred during the Dust Bowl years (Figure S4).

It is worth noting as well, that annual average T show similarly high values during the Dust Bowl years in the 1930s and 1940s, but also display significant increasing trends through time after 1960 (Figure S3). Thus impacts to annual average T and daily maximum T extremes could prove to be quite different at different times in the future.

In addition to changing summer precipitation, atmospheric chemistry could play a role in suppressing increases in maximum daily temperatures (e.g. increasing particulate concentrations may increase albedo, resulting in net reductions in solar radiation). High-resolution climate model simulations that include atmospheric chemistry are needed to explore these potential negative feedbacks on extreme high temperatures.

The number of extreme cold days (Tmin < -15 °C (5 °F)) per year is projected to decrease with warming (Figure S6). In the northern part of the domain, for example, the average number of extreme cold days per year declines from about 15 for baseline conditions to 5 for the 2080s RCP8.5 scenario.

*4.1.2 Precipitation Changes*

For IN, P is projected to increase substantially in winter and spring for most scenarios (Figure 1 bottom panels). Projected changes in summer and fall P, by comparison, show relatively small decreases and there is not a strong consensus between models for wetter or drier conditions in these seasons. This seasonal pattern of changing P increases in intensity through time in the scenarios. Projected annual changes in P are generally positive, and by the 2080s for the RCP8.5 scenario all GCMs show increases in annual P over IN.

At the macro scale, meaningful patterns of spatial variability for changes in P are not readily apparent, except during fall, which shows somewhat drier conditions in southern IN and wetter conditions in northern IN. Spring also shows a weak pattern of wetter conditions in the north, but all changes in P over IN are positive in this case. Note, however, that the spatial standard deviation of delta P, calculated at the grid-cell scale, is often comparable or larger in magnitude to the average change in P itself. Table 2B summarizes percent changes in P for each season, emissions scenario, and time period.

Warming over the state is accompanied by a decreasing fraction of Nov-Mar P falling as snow (Figure 4). By the 2080s for RCP8.5, snow is infrequent in southern IN (little snowfall even in midwinter), whereas northern IN still receives substantial snowfall from Nov-Mar, albeit much less snowfall during this period than for the historical baseline conditions.

Figure S7 shows substantial reductions in the number of events with more than 5 mm of snow water equivalent (SWE), which is approximately equal to 5 cm (2 inches) of snowfall. This

threshold was chosen because snowfall greater than this amount typically requires plowing to clear streets, and shoveling or snowblowing to clear sidewalks. This reduction in the number of days with more than 2 inches of snowfall therefore implies fewer resources would be required for plowing (municipalities and businesses) and shoveling or snowblowing (individuals).

Although GCMs are not capable of explicitly simulating small-scale convective storms that often lead to annual extremes (see discussion of dynamical downscaling above), we nonetheless argue that simulations of heavy precipitation from GCMs, when coupled with probability-distribution based bias-correction approaches, are likely to represent meaningful changes, especially in cool season when projected precipitation changes are largest and convective storms are relatively rare. Figure S8 shows increases in the ensemble average number of days per year with more than 25mm of precipitation. Some of the fine-scale patterns on the plot are caused by gridding artifacts (i.e. fewer extreme events are shown between stations due to averaging from multiple stations; Ensor and Robeson 2008), but the large-scale pattern nonetheless shows substantial increases of 3 to 4 days per year in the number of days of heavy precipitation. Analysis for a 50mm P threshold (not shown) yielded qualitatively similar results. Results for selected urban centers in IN are shown in Table S2.

One caveat associated with this analysis is that the potential for increasing frequency of convective storms in mid-winter (e.g., on Feb 20, 2018 in IN) is not well captured in GCM simulations due to problems with spatial resolution. Similarly, changes in lake-effect snow, which are a function of both lake conditions (e.g., surface T, ice cover) and atmospheric conditions (e.g., frequency, intensity, and duration of arctic air outbreaks) are not well captured by GCMs, many of which do not even resolve the Great Lakes (Byun and Hamlet 2018). Simulations from high-resolution regional-scale climate models coupled to lake hydrodynamic

models are needed to better address changes in these two important impact pathways (Sharma et al. 2018).

### *4.2 Length of Frost-Free Growing Season and USDA Hardiness Zone Maps*

The average length of the frost-free growing season increases substantially in the projected future climate (Figure S9). By the 2020s, the length of the frost-free growing season increases by about 10 days overall and there are only minor differences between the RCP4.5 and 8.5 scenarios. By the 2080s, the RCP4.5 scenario shows increases in growing season of 20 to 30 days whereas the RCP8.5 scenario shows increases of 30 to 50 days.

Changes in ensemble-average USDA Plant Hardiness Zones (Figure S10), which are based on expected extreme winter low temperatures, show typical increases of about two half zones by the 2080s over much of IN, i.e. from zone 6a for the baseline climate to zone 7a for the 2080s RCP8.5 scenario. Note that zone 7a indicated for northern IN for the 2080s RCP8.5 scenario is the same hardiness zone as southern IN for the historical climate. Zone 7b, which currently occurs in northern Alabama, begins to appear in extreme southern Indiana in the 2080s RCP8.5 scenario.

### *4.3 Impacts to Energy Demand for Space Cooling and Heating*

Figure S11 and S12 show projected changes in cooling degree days (° F) (relative to 75 °F) and heating degree days (relative to 68 °F) respectively. Cooling degree days increase by approximately a factor of 4 for the 2080s RCP8.5 scenarios, and heating degree days decline by about 30%. These changes imply a net *decrease* in overall energy demand for space heating and cooling, however, due to the relatively large number of heating degree days in IN, and a typically higher coefficient of performance (COP) for electrical A/C equipment (COP ~2.5) as compared

to electrical space heating (COP ~1.0) (see Raymond et al. in review, and Hamlet et al. 2010 for additional discussion). Note that for heating degree days, the 2080s RCP8.5 values in northern IN are comparable to the historical values in southern IN; whereas, for cooling degree days, the 2080s RCP8.5 projections in northern IN are much higher than the historical values in southern IN. This difference reflects the fact that the largest *T* changes are projected during summer.

### *4.4 Constructing Spatial Analogues to IN's Projected Future Climate*

Spatial analogues for IN's projected future climate were constructed by finding the closest match for the projected future IN climate to the current climate in other parts of the country. These analogs were based on the gridded 1981-2010 mean T and P values from the PRISM data sets (Daly et al. 2008). For each PRISM grid-point, winter (DJF) and summer (JJA) means of T and P were used to find the minimum "distance" of the projected climate to the current climate using a six-element vector (T and P for each of the three months). Stratifying the data by winter and summer shows the distinct seasonal changes that are likely to occur in IN while allowing for closer spatial analogs to be found. Figure S13 and S14 show winter and summer analogs for the 2050s and 2080s respectively for the two greenhouse gas concentration scenarios. In winter, IN's projected future climate approximates the current climate of the mid-Atlantic states (Figure S13), whereas in summer IN's projected future climate approximates the current climate in areas substantially farther to the south and west (Figure S14). By the 2080s for the RCP8.5 scenario, for example, IN's projected future climate in summer is comparable to the current climate of southeastern Texas.

## *5 Conclusions*

The state of IN is projected to experience profound changes in climate by 2100.For the 2080s RCP 8.5 climate change scenarios presented here, Indiana's climate will shift to one that is similar to the current climate for the mid-Atlantic states in winter and similar to the current climate of southeaster Texas for summer. Large changes in T are projected for IN, which will have important impacts on urban environments (Reynolds et al. in review), human health (Filippelli et al. in review), energy (Raymond et al. in review), agriculture (Bowling et al., in preparation), forests (Phillips et al. in review), and water resources (Cherkauer et al., in preparation). Substantial changes in traditional winter recreation opportunities are also projected due to systematic loss of snow and ice cover in the future (Chin et al. 2018). Changes in extreme high T are most clearly linked to drought in both the historical record and future projections, which implies that impacts to extreme high T may be quite variable in time in response to relatively uncertain changes in summer P in the projections. That is, unusually dry decades in the future may show extreme heat impacts, whereas less drought-prone decades may be substantially cooler. Unusually wet conditions in summer are also associated with very warm conditions in the projections, however, which suggests that warm, moist air advected from the south may be another important cause of extreme heat and humidity in the projections.

Reductions in energy demand for space heating due to warming, however, will likely be a benefit to many (see also Raymond et al., in review), and reductions in snowfall may reduce costs of snow removal for municipalities, businesses, and individuals. Projected changes in P, particularly its seasonality, are also substantial, with a projected 25-30% increase in winter and spring P by the 2080s for the RCP8.5 scenario. By the 2080s all climate models in the RCP8.5 CMIP5 archive show increases in annual P over IN, but increasing evapotranspiration with warming could reduce the net effects on soil moisture (Cherkauer et al., in review). Changes in

summer convective storms cannot be captured by large-scale climate models like the ones used in this study, but increasing P intensity from convective storms has already emerged in the historical record as an important impact pathway for cities and these trends are projected to continue to increase with future warming (e.g., Prein et al. 2018). We also hypothesize that convective storms will be increasingly observed in winter as warming progresses. Coincident increases in P as rain, accompanied by loss of snow cover in winter and spring, will likely impact water quality and erosion in agricultural areas (Bowling et al., in preparation) and may lead to elevated soil moisture and increased flooding in winter and spring in IN rivers (Cherkauer et al., this issue; Byun et al. 2018). Lake-effect snow is hypothesized to increase in the next several decades due to warmer lake surface temperatures and longer ice-free conditions, but towards the end of the 21st century T may become too warm, resulting in conversion from lake-effect snow to lake-effect rain, especially in the shoulder seasons. Regional-scale climate models dynamically coupled to lake hydrodynamic models are needed to evaluate these impact pathways in a more physically based manner.

**Acknowledgements:**

This paper is a contribution to the Indiana Climate Change Impacts Assessment (INCCIA). The INCCIA is organized and financially supported by the Purdue Climate Change Research Center.

**References:**

Bowling, L., Beckerman, J., Brouder, S., Buzan, J., Cherkauer, K., Doering, O., Dukes, J., Ebner, P., Frankenberger, J., Gramig, B., Kladivko, E., Lee., C., Volenec, J, and C. Weill (in preparation). Agricultural Impacts of Climate Change in Indiana and Potential Adaptations.

Byun, K. and A.F. Hamlet, 2018: Projected Changes in Future Climate over the Midwest and Great Lakes Region Using Downscaled CMIP5 Ensembles, International Journal of Climatology, (in press).

Cherkauer, K.A., Bowling, L., Chaubey, I., Chin, N., Ficklin, D., Kines, S., Lee, C., Pignotti, G., Rahman, S., Singh, S., Valappil, F., and T. Williamson. (in preparation). Climate change impacts and strategies for adaptation for water resource management in Indiana. Climatic Change

Chiu, C.-M., A. F. Hamlet, K. Byun, 2018: An Improved Meteorological Driving Data Set for the Great Lakes Region Incorporating Precipitation Gauge Undercatch Corrections (in review)

Daly C, Halbleib M, Smith JI, Gibson WP, Doggett MK, Taylor GH, Curtis J, Pasteris PP (2008) Physiographically sensitive mapping of climatological temperature and precipitation across the conterminous United States. Int J Climatol 28:2031–2064. https://doi.org/10.1002/joc.1688

Ensor, L. A., S. M. Robeson, 2008: Statistical characteristics of daily precipitation: comparisons of gridded and point datasets. *Journal of Applied Meteorology and Climatology*, *47*(9), 2468-2476.

Hamlet, A.F., S.Y. Lee, K.E.B. Mickelson, M.M. Elsner, 2010: Effects of projected climate change on energy supply and demand in the Pacific Northwest and Washington State, Climatic Change, 102 (1-2), doi: 10.1007/s10584-010-9857-y

Hamlet, A. F., M. M. Elsner, G. Mauger, S.-Y. Lee, I. Tohver, and R. a. Norheim, 2013: An Overview of the Columbia Basin Climate Change Scenarios Project : Approach, Methods, and Summary of Key Results. Atmosphere-Ocean, 51, 392–415, doi:10.1080/07055900.2013.819555.

IPCC, 2013, Climate Change 2013: The Physical Basis. Contribution of Working Group 1 to the Fifth Assessment Report of the IPCC, Cambridge University Press, 1535pp.

Liu, C., Ikeda, K., Rasmussen, R., Barlage, M., Newman, A.J., Prein, A.F., Chen, F., Chen, L., Clark, M., Dai, A. and Dudhia, J., 2016: Continental-scale convection-permitting modeling of the current and future climate of North America. Climate Dynamics, pp.1-25

Moss, R.; Mustafa Babiker; Sander Brinkman; Eduardo Calvo; Tim Carter; Jae Edmonds; Ismail Elgizouli; Seita Emori; Lin Erda; Kathy Hibbard; Roger Jones; Mikiko Kainuma; Jessica Kelleher; Jean Francois Lamarque; Martin Manning; Ben Matthews; Jerry Meehl; Leo Meyer; John Mitchell; Nebojsa Nakicenovic; Brian O'Neill; Ramon Pichs; Keywan Riahi; Steven Rose; Paul Runci; Ron Stouffer; Detlef van Vuuren; John Weyant; Tom Wilbanks; Jean Pascal van Ypersele & Monika Zurek, 2008: Towards New Scenarios for Analysis of Emissions, Climate Change, Impacts, and Response Strategies, Geneva: Intergovernmental Panel on Climate Change. p. 132.

Mueller ND, Butler EE, McKinnon KA, Rhines A, Tingley M, Holbrook NM, Huybers P (2016) Cooling of US Midwest summer temperature extremes from cropland intensification. Nat Clim Chang 6(3):317–322

Phillips, R.P., Brandt, L., Polly, D., Zollner, P., Saunders, M.R., Clay, K., Iverson, L., and Fei, S. (In review). Towards an improved understanding of the ecological and economic consequences of climate change for Indiana forests. Climatic Change. Climatic Change

Prein, A.F., C. Liu, K. Ikeda, S. B. Trier, R. M. Rasmussen, G. J. Holland, M. P. Clark, 2018: Increased rainfall volume from future convective storms in the US, Nature Climate Change, (7): 880-884

Raymond L, Gotham D, McClain W, Mukherjee S, Nateghi R, Preckel PV, Schubert P, Singh S, Wachs L. Projected climate change impacts on Indiana's energy demand and supply. Climatic Change (in press)

Reynolds, H.L, Brandt, L., Fischer, B.C., Hardiman, B.S., Moxley, D.J., Sandweiss, E., Speer, J., and S. Fei. (in review). Implications of climate change for managing urban green infrastructure in Indiana. Climatic Change. Climatic Change

Rupp DE, Abatzoglou JT, Hegewisch KC, Mote PW (2013) Evaluation of CMIP5 20th century climate simulations for the Pacific Northwest USA. J Geophys Res Atmos 118(10):884–10,906. https://doi.org/10.1002/jgrd.50843

Sharma, A., A. F. Hamlet, H. J. S. Fernando, C. E. Catlett, D. E. Horton, V. R. Kotamarthi, D. A. R. Kristovich, A. I. Packman, J. L. Tank, D. J. Wuebbles, 2018: The need for an integrated

land-lake-atmosphere modeling system, exemplified by North America's Great Lakes region, Earth's Future, (in review)

Schoof, J. T. and S. M. Robeson, 2016: Projecting changes in regional and local climate extremes in the United States. *Weather and Climate Extremes*, 11, 28-40.

Smith, S. J., & Mizrahi, A. 2013: Near-term climate mitigation by short-lived forcers. *Proceedings of the National Academy of Sciences, 110*(35), 14202-14206.

Taylor, K. E., R. J. Stouffer, and G. A. Meehl, 2012: An overview of CMIP5 and the experiment design. Bull. Am. Meteorol. Soc., 93, 485–498, doi:10.1175/BAMS-D-11-00094.1.

Tohver, I. M., A. F. Hamlet, and S. Y. Lee, 2014: Impacts of 21st-Century Climate Change on Hydrologic Extremes in the Pacific Northwest Region of North America. J. Am. Water Resour. Assoc., 50, 1461–1476, doi:10.1111/jawr.12199.

USGCRP (2017) In: Wuebbles DJ, Fahey DW, Hibbard KA, Dokken DJ, Stewart BC, Maycock TK (eds) Climate science special report: fourth national climate assessment, volume I. U.S. Global Change Research Program, Washington, DC, p 470

Vose, R. S., Applequist, S., Squires, M., Durre, I., Menne, M. J., Williams Jr, C. N., ... & Arndt, D., 2014: Improved historical temperature and precipitation time series for US climate divisions. Journal of Applied Meteorology and Climatology, 53(5), 1232-1251.

Winkler, J. a, R. W. Arritt, and S. C. Pryor, 2012: Climate Projections for the Midwest: Availability, Interpretation and Synthesis. US Natl. Clim. Assess. Midwest Tech. Input Rep., 24, doi:9781610915113.

Wood, A.W., Maurer, E.P., Kumar, A. and D.P. Lettenmaier, 2002: Long range experimental hydrologic forecasting for the eastern U.S. Journal of Geophysical Research, 107(D20), 4429, doi:10.1029/2001JD000659.

Wood, A. W., L. R. Leung, V. Sridhar, and D. P. Lettenmaier, 2004: Hydrologic implications of dynamical and statistical approaches to downscaling climate model outputs, Climatic Change, 62, 189–216, doi:10.1023/B:CLIM.0000013685.99609.9e.

***Tabes and Figures:***

**Table 1**. Overview of Data Processing Approaches Used to Generate Figures and Tables.

| | Overview of Approach | Examples | Notes |
|---|---|---|---|
| Type I | Data are analyzed as a time series for each grid cell, and the results of the time series analysis (a single value for each cell) are then presented as a spatial map over some domain of interest. | Mean, variance, change relative to some base period, ratios of snow to P, extreme values, ensemble mean, etc. extracted from the time series for each cell and plotted as a map (color bar or contour plot). | In this paper the domain of interest is mostly IN, but can be any subset of this domain. |
| Type II | Data are averaged in space for some domain of interest for each time step, and these single values for each time step are then plotted as a line graph with time in the X axis. | Domain average values of P or T plotted as an annual time series to show the effects of historical variability. Ranges can be shown by processing multiple GCMs as a separate time series and then statistically analyzing | Any time step of interest can be used, but typically monthly or annual values are plotted. |

| | | | |
|---|---|---|---|
| | | the ensemble at each time step (e.g. Figure S1). | |
| Type III | Data are aggregated and/or averaged in space and time to produce a single value for each space/time data set. A single value may also be extracted for each calendar month, to produce a composite mean plot of the seasonal cycle. | Percent change in P for the Midwest for a group of GCMs to produce a range of values (e.g. Figure S2). Monthly domain-average changes in T or P for a group of GCMs (e.g. Figure 1). | |

**Table 2**. **A)** Projected annual and seasonal temperature changes (°C) over Indiana. The first value is the spatially averaged, ensemble mean temperature change. The value in parentheses is the spatial standard deviation of the ensemble mean delta T over Indiana. **B)** Projected annual and seasonal precipitation changes (%) over Indiana. The first value is the spatially-averaged, ensemble-mean, percent change in P. The value in parentheses is the spatial standard deviation over Indiana.

**A)**

| GHG Scenarios | Future Periods | Annual (°C) | Spring (°C) | Summer (°C) | Fall (°C) | Winter (°C) |
|---|---|---|---|---|---|---|
| **RCP4.5** | **2020s** | 1.63 (0.10) | 1.44 (0.11) | 1.68 (0.10) | 1.86 (0.10) | 1.56 (0.11) |
| | **2050s** | 2.71 (0.10) | 2.34 (0.12) | 2.83 (0.11) | 2.82 (0.10) | 2.86 (0.13) |
| | **2080s** | 3.29 (0.11) | 2.81 (0.11) | 3.70 (0.11) | 3.46 (0.12) | 3.20 (0.14) |
| **RCP8.5** | **2020s** | 1.73 (0.10) | 1.36 (0.12) | 1.85 (0.10) | 1.80 (0.10) | 1.89 (0.12) |
| | **2050s** | 3.44 (0.11) | 2.85 (0.12) | 3.87 (0.12) | 3.59 (0.11) | 3.44 (0.17) |
| | **2080s** | 5.60 (0.13) | 4.54 (0.12) | 6.56 (0.13) | 6.08 (0.13) | 5.22 (0.26) |

**B)**

| GHG Scenarios | Future Periods | Annual (%) | Spring (%) | Summer (%) | Fall (%) | Winter (%) |
|---|---|---|---|---|---|---|
| **RCP4.5** | **2020s** | 1.78 (1.72) | 3.75 (1.88) | -1.44 (1.84) | -3.89 (2.91) | 8.69 (2.42) |
| | **2050s** | 6.05 (1.67) | 12.70 (1.81) | -1.83(1.78) | -2.35 (3.34) | 15.67 (2.71) |
| | **2080s** | 5.33 (2.13) | 10.15 (2.17) | -3.29 (2.11) | -2.72 (3.08) | 17.20 (3.01) |
| **RCP8.5** | **2020s** | 2.77 (1.74) | 7.35 (1.70) | -3.45 (1.89) | -2.97 (3.29) | 10.15 (2.48) |
| | **2050s** | 7.70 (1.74) | 15.67 (2.14) | -3.43 (1.89) | -1.76 (3.03) | 20.33 (2.76) |
| | **2080s** | 9.97 (2.07) | 17.24 (2.52) | -7.60 (2.10) | -1.81 (2.98) | 32.06 (2.99) |

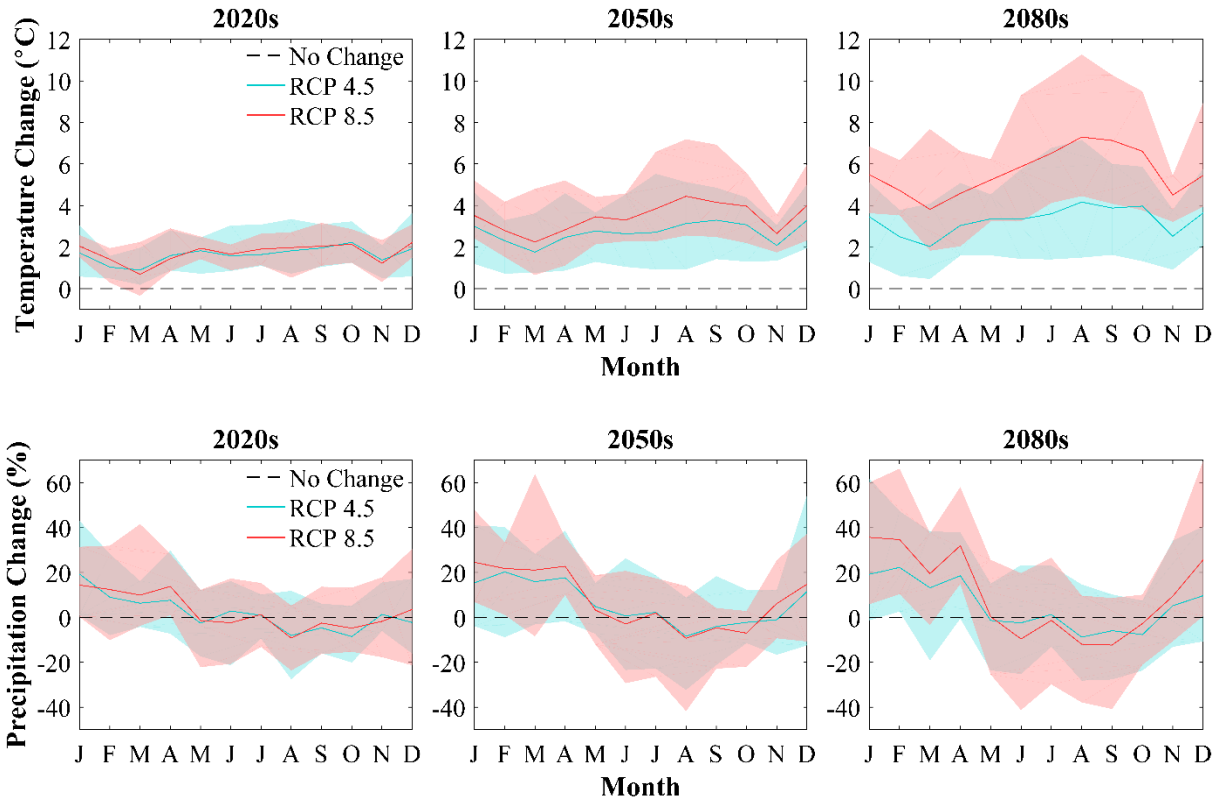


**Figure 1.** Top Panels: Monthly changes in T averaged over IN relative to a 1971-2000 baseline for the 2020s (2011-2040), 2050s (2041-2070), and 2080s (2071-2100) with ensemble spread shown separately for two emissions scenarios (RCP4.5 and RCP8.5). Bottom Panels: Monthly % changes in P relative to a 1971-2000 baseline with ensemble spread for the 2020s, 2050s, 2080s RCP4.5 RCP8.5

[Method: Type III, one value per calendar month averaged in time and space for each GCM scenario, and plotted as a range and central tendency for each month].

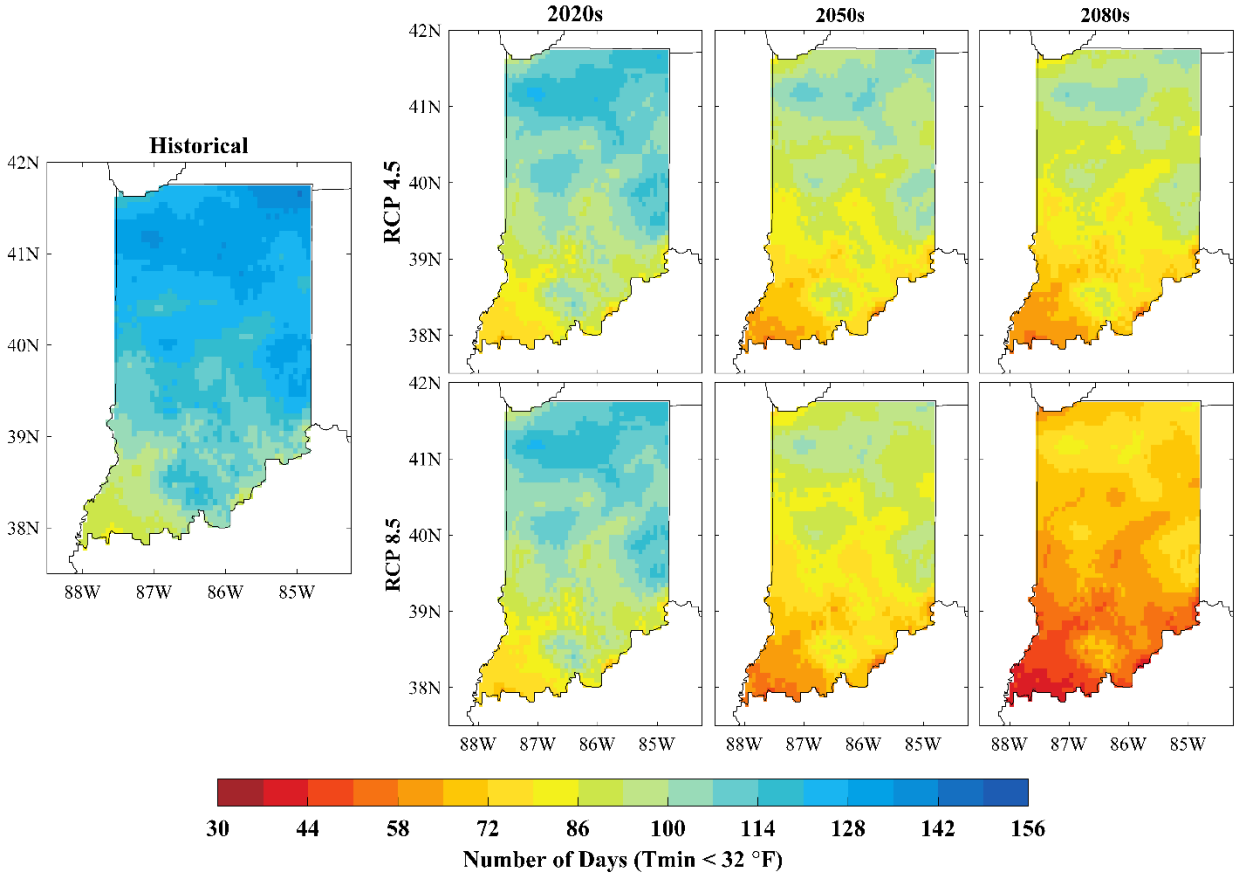


**Figure 2.** Map of annual number of frost days (Tmin < 0 °C (32 °F)). Seven panels: Historical (1915-2013) and 2020s, 2050s, 2080s with RCP4.5 and RCP8.5 [Method: Type I, ensemble mean annual number of frost days for each cell].

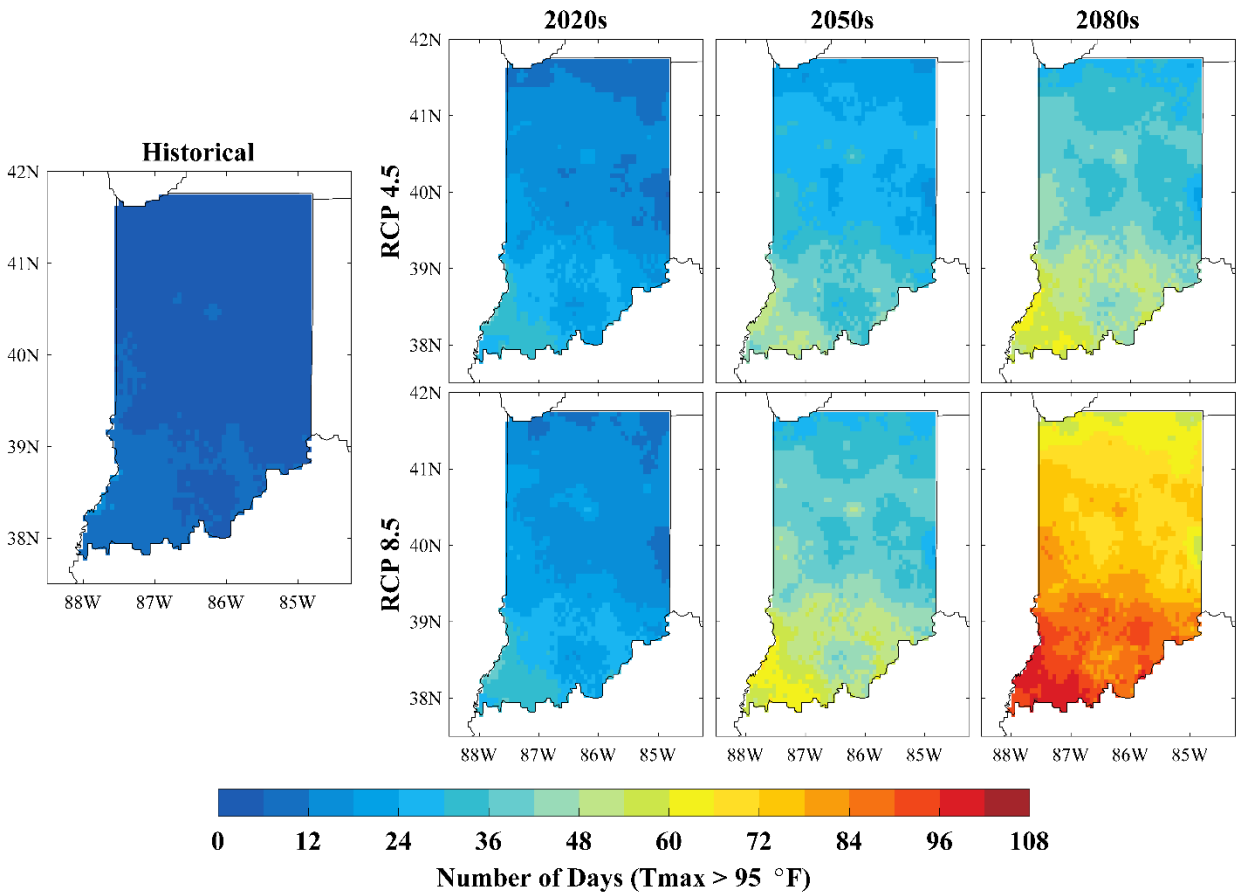


**Figure 3.** Annual number of days with extreme hot temperatures (Tmax > 35 °C (95 °F)). Seven panels: Historical (1915-2013) and 2020s, 2050s, 2080s with RCP4.5 and RCP8.5 [Method: Type I, ensemble mean number of extreme hot days].

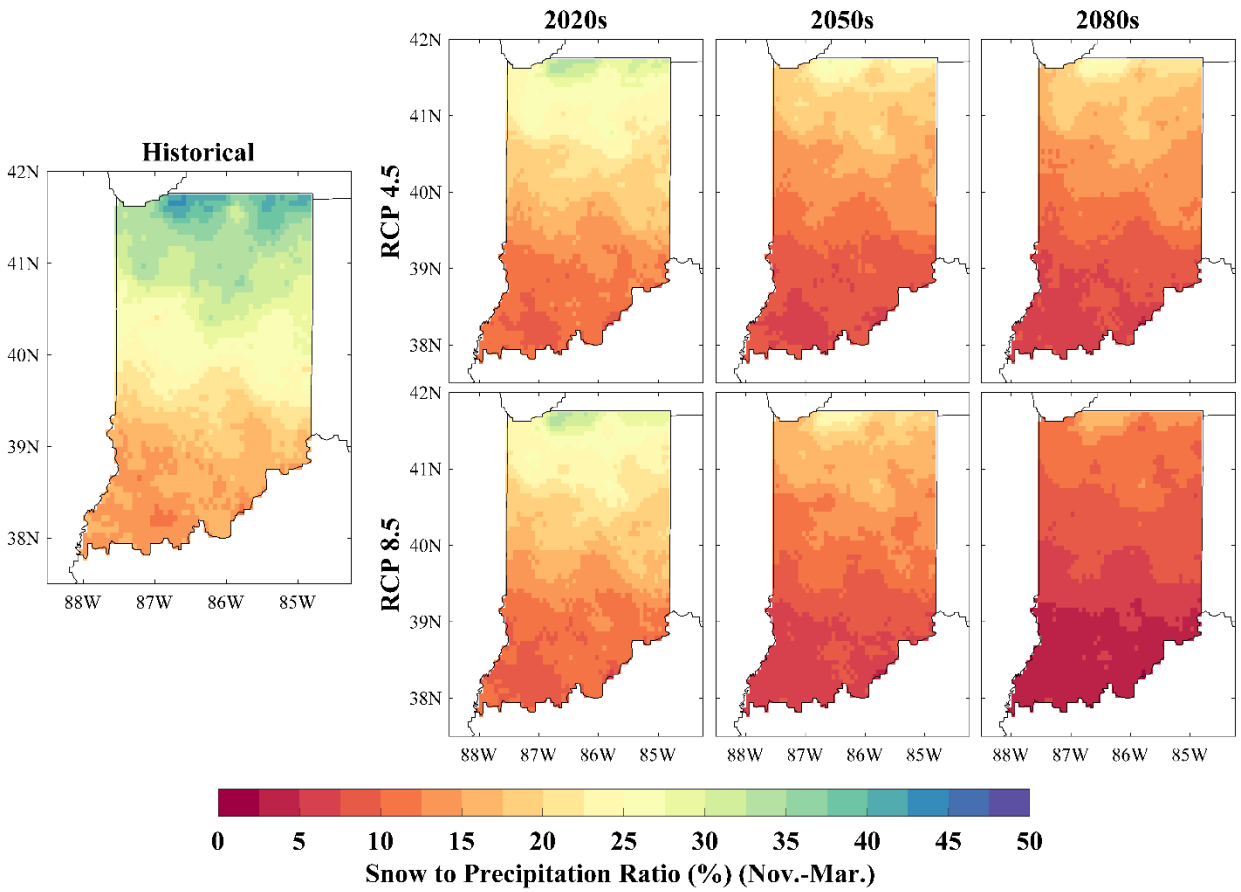


**Figure 4.** Ensemble-average, long-term-mean fraction of Nov-Mar P as snow. Seven panels: Historical (1915-2013) and 2020s, 2050s, 2080s for the RCP4.5 and RCP8.5 emissions scenarios.

***Supplemental Tables and Figures***

**Table S1.** Historical baseline and RCP 8.5 2080s future projections of the number extreme hot days (Tmax > 35 °C (95 °F)) per year for several Indiana urban centers.

| **Urban Center** | # Historical Hot Days | # 2020s RCP 8.5 Hot Days | # 2050s RCP 8.5 Hot Days | # 2080s RCP 8.5 Hot Days |
|---|---|---|---|---|
| Gary | 4.9 | 14.0 | 30.6 | 61.7 |
| South Bend | 3.0 | 11.0 | 27.9 | 58.6 |

| | | | | |
|---|---|---|---|---|
| Fort Wayne | 2.5 | 11.8 | 30.4 | 63.5 |
| Indianapolis | 4.0 | 16.3 | 38.8 | 75.2 |
| Muncie | 3.0 | 14.6 | 36.9 | 73.0 |
| Brownstown | 6.2 | 26.2 | 52.2 | 89.9 |
| Evansville | 10.5 | 34.3 | 61.4 | 98.2 |
| Bloomington | 6.3 | 24.4 | 49.8 | 87.7 |
| Terre Haute | 7.5 | 21.5 | 44.2 | 80.5 |
| Lafayette | 4.9 | 16.3 | 37.6 | 72.3 |
| New Albany | 8.2 | 31.0 | 58.1 | 96.4 |

**Table S2.** Historical baseline and RCP 8.5 future projections of the number of days with more than 25mm of precipitation for several Indiana urban centers.

| **Urban Center** | # Historical Days (P>25mm) | # 2020s RCP 8.5 Days (P>25mm) | # 2050s RCP 8.5 Days (P>25mm) | # 2080s RCP 8.5 Days (P>25mm) |
|---|---|---|---|---|
| Gary | 9.4 | 9.5 | 10.3 | 10.7 |
| South Bend | 8.6 | 9.0 | 9.8 | 10.4 |
| Fort Wayne | 7.1 | 7.8 | 8.6 | 9.3 |
| Indianapolis | 9.9 | 10.7 | 11.7 | 12.2 |
| Muncie | 9.5 | 10.5 | 11.5 | 12.1 |
| Brownstown | 11.9 | 12.3 | 13.6 | 14.1 |
| Evansville | 12.5 | 13.0 | 14.4 | 14.7 |
| Bloomington | 14.8 | 15.4 | 16.5 | 16.8 |
| Terre Haute | 11.7 | 11.8 | 12.9 | 13.2 |
| Lafayette | 8.8 | 10.1 | 11.2 | 11.6 |
| New Albany | 12.8 | 13.0 | 14.3 | 14.9 |

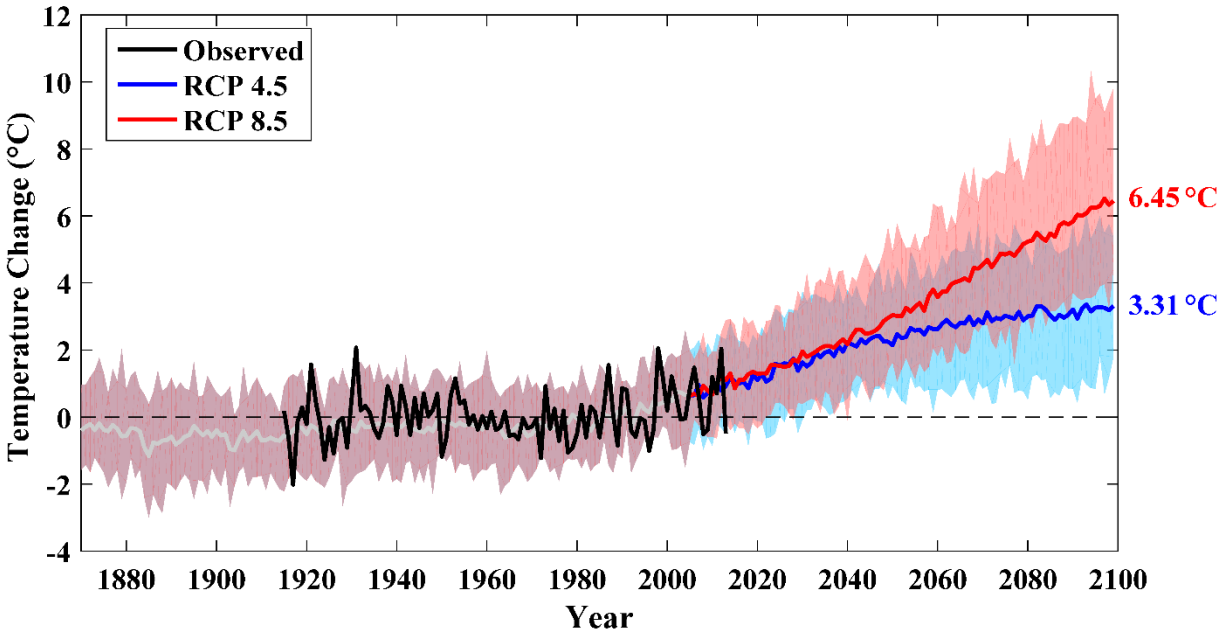


**Figure S1**. Trajectory of annual mean temperature change over the Midwest region relative to the annual mean temperature for the historical baseline period (1971-2000). Each shaded bound represents 95% confidence interval (2.5$^{th}$ percentile to 97.5$^{th}$ percentile) and solid lines display the ensemble mean of 31 bias corrected GCMs results. Heavy black line shows domain-averaged annual temperature from historical observations (1915-2013). (Source: Byun and Hamlet 2018.)

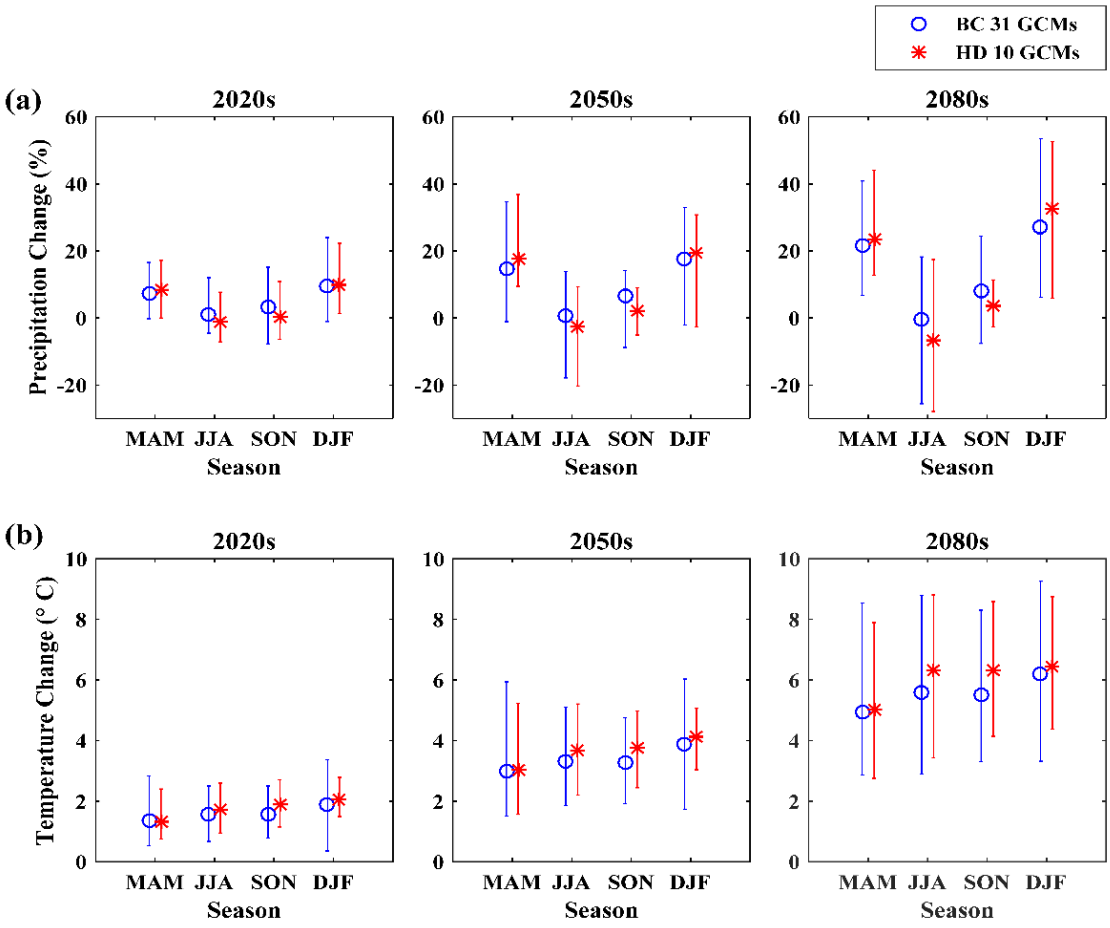


**Figure S2.** Projected seasonal changes relative to 1971-2000 in (a) precipitation (%) and (b) temperature (°C) from 31 bias corrected coarse-resolution GCMs (blue) and 10 HD downscaled GCMs (red) based on RCP 8.5. Each range bar is bounded by the minimum and maximum values, and the marker represents the mean of all GCMs in each grouping. (Source: Byun and Hamlet 2018.)

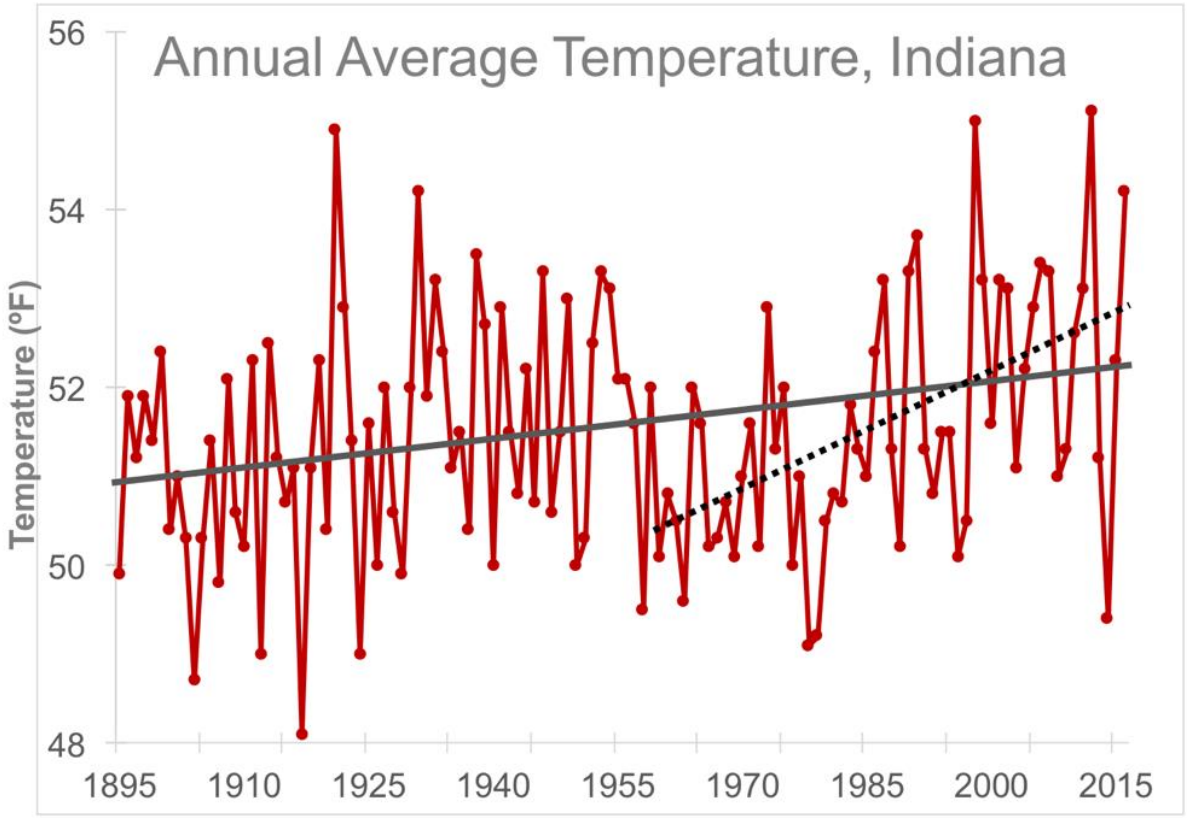


**Figure S3.** Statewide annual average temperature for Indiana from 1895 – 2016. Black solid line shows the increasing trend in annual temperature (0.1°F/decade) for the period of record (1895-2016). The black dotted line shows the temperature trend since 1960 (0.4°F"/decade). Data are from the NOAA Climate At A Glance Database, accessed October 2017. Data are further described in Vose et al., 2014. (Vose, R. S., Applequist, S., Squires, M., Durre, I., Menne, M. J., Williams Jr, C. N., ... & Arndt, D., 2014: Improved historical temperature and precipitation time series for US climate divisions. Journal of Applied Meteorology and Climatology, 53(5), 1232-1251)

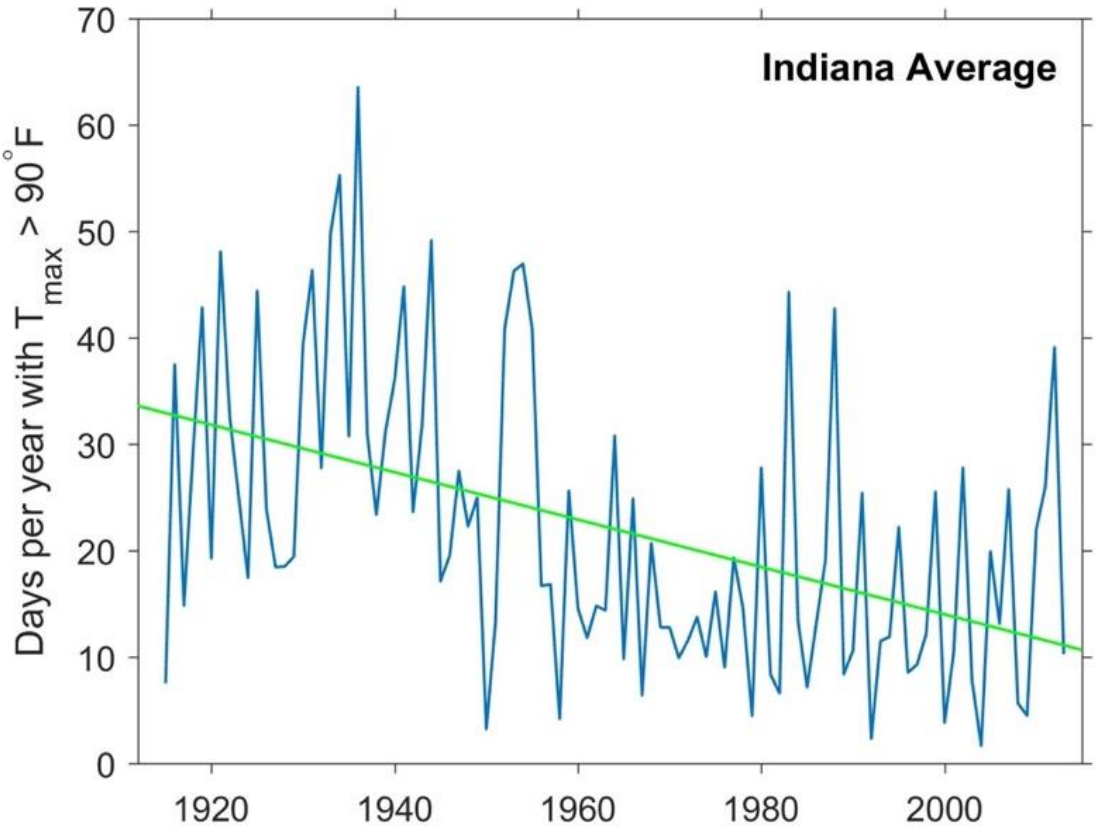


**Figure S4.** The number of days per year when the maximum daily temperature averaged over IN is above 90°F (blue line). The linear trend over the period of record from 1915-2013 is shown in green.

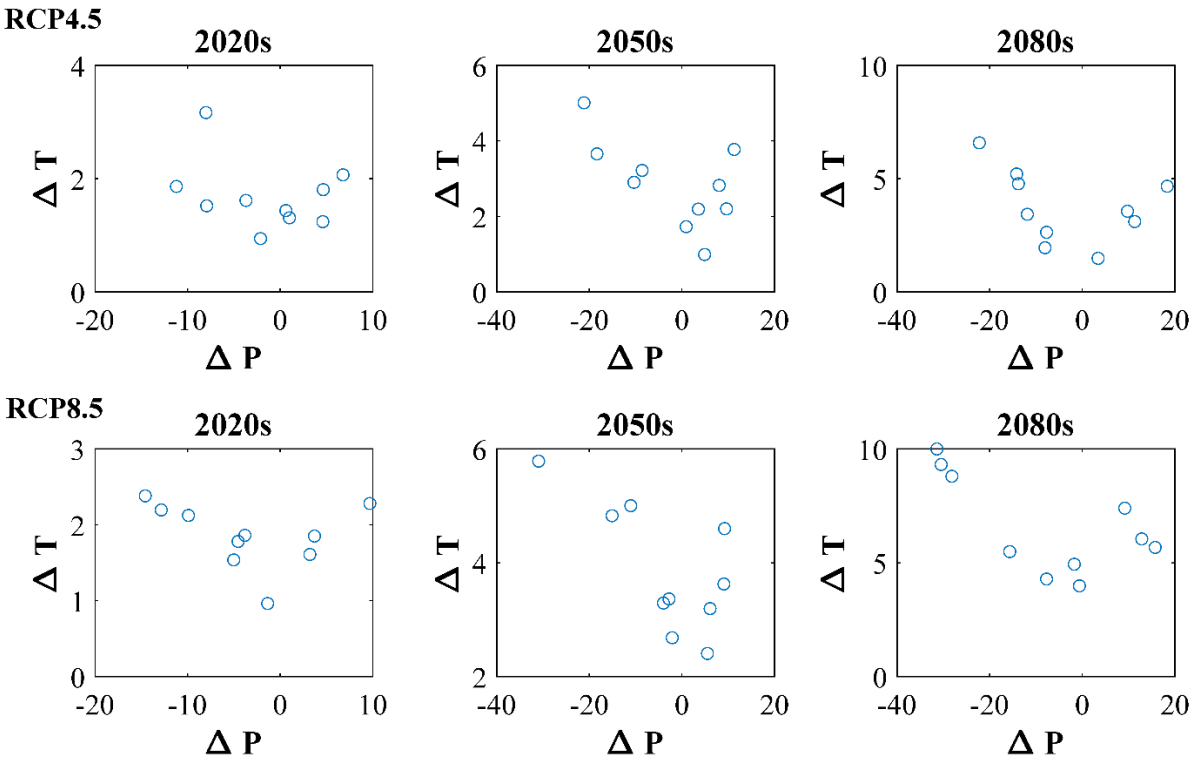


**Figure S5.** Scatter plots of summer delta T vs. delta P for 10 climate model projections, three time periods, and two greenhouse gas concentration scenarios.

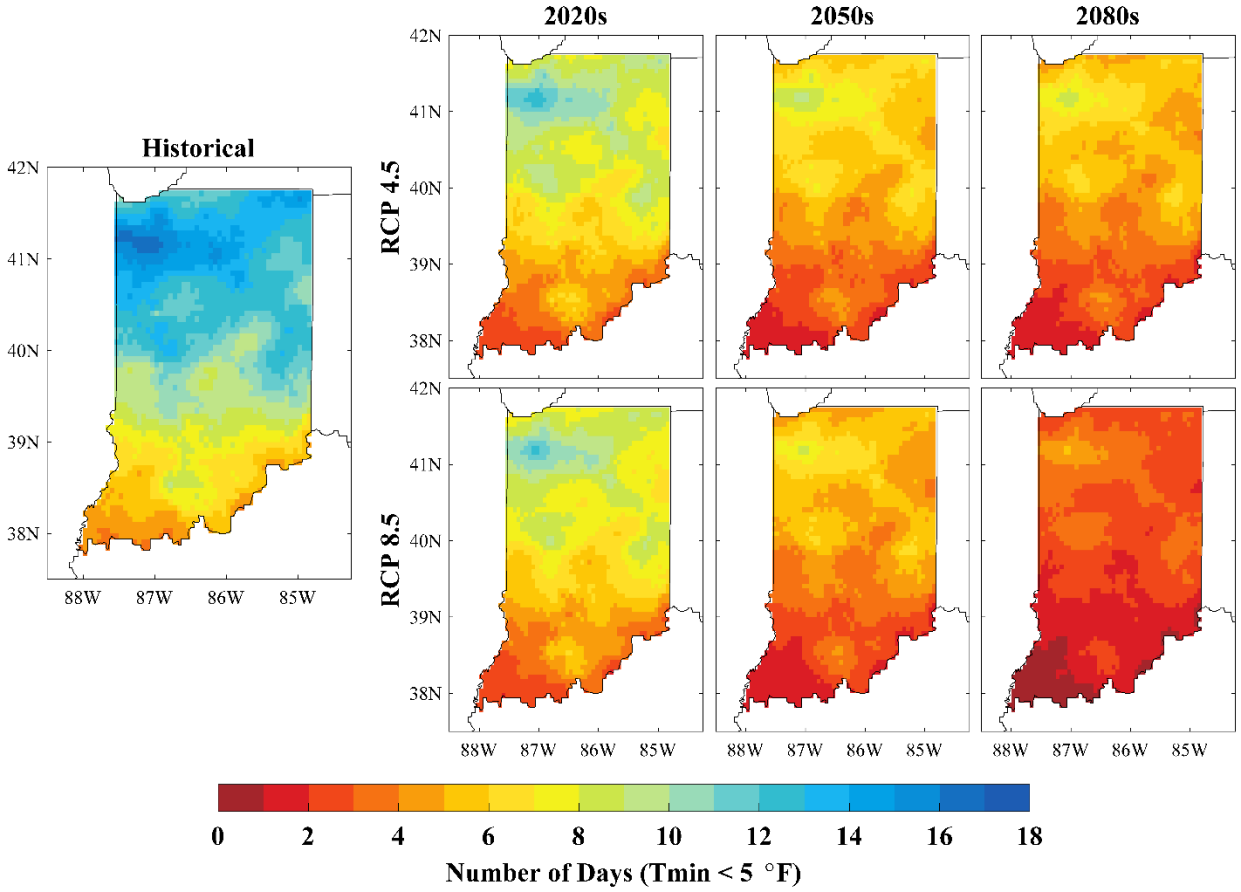


**Figure S6.** Annual number of days with extreme cold temperatures (Tmin < -15 °C (5 °F)). Seven panels: Historical (1915-2013) and 2020s, 2050s, 2080s with RCP4.5 and RCP8.5 [Method: Type I, annual number of extreme cold days].

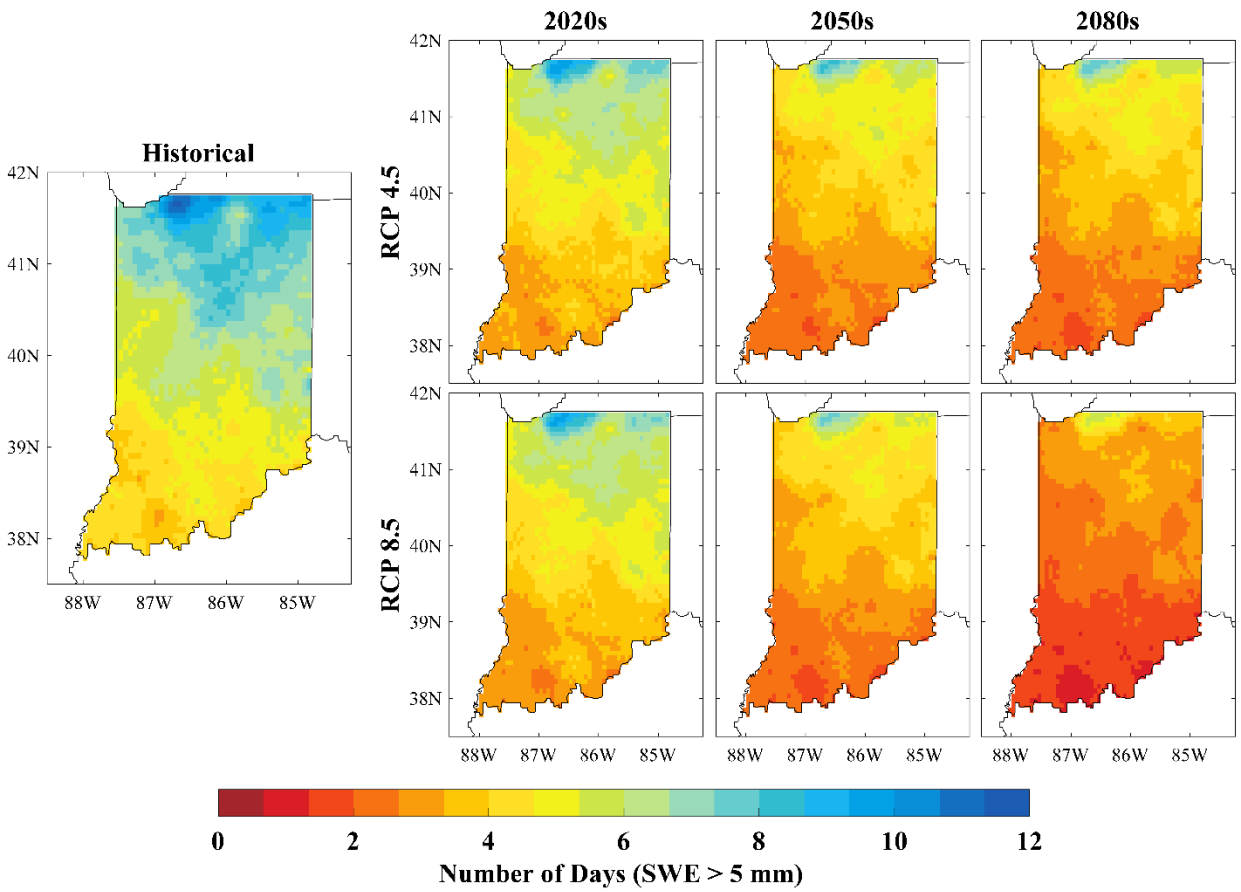


**Figure S7.** Ensemble-average, long-term mean number of days with more than 5 mm of SWE (~2 in of snow). Seven panels: Historical (1915-2013) and 2020s, 2050s, 2080s for the RCP4.5 and RCP8.5 emissions scenarios. [Method: Type I, ensemble average of annual number days with more than 5 mm of SWE]

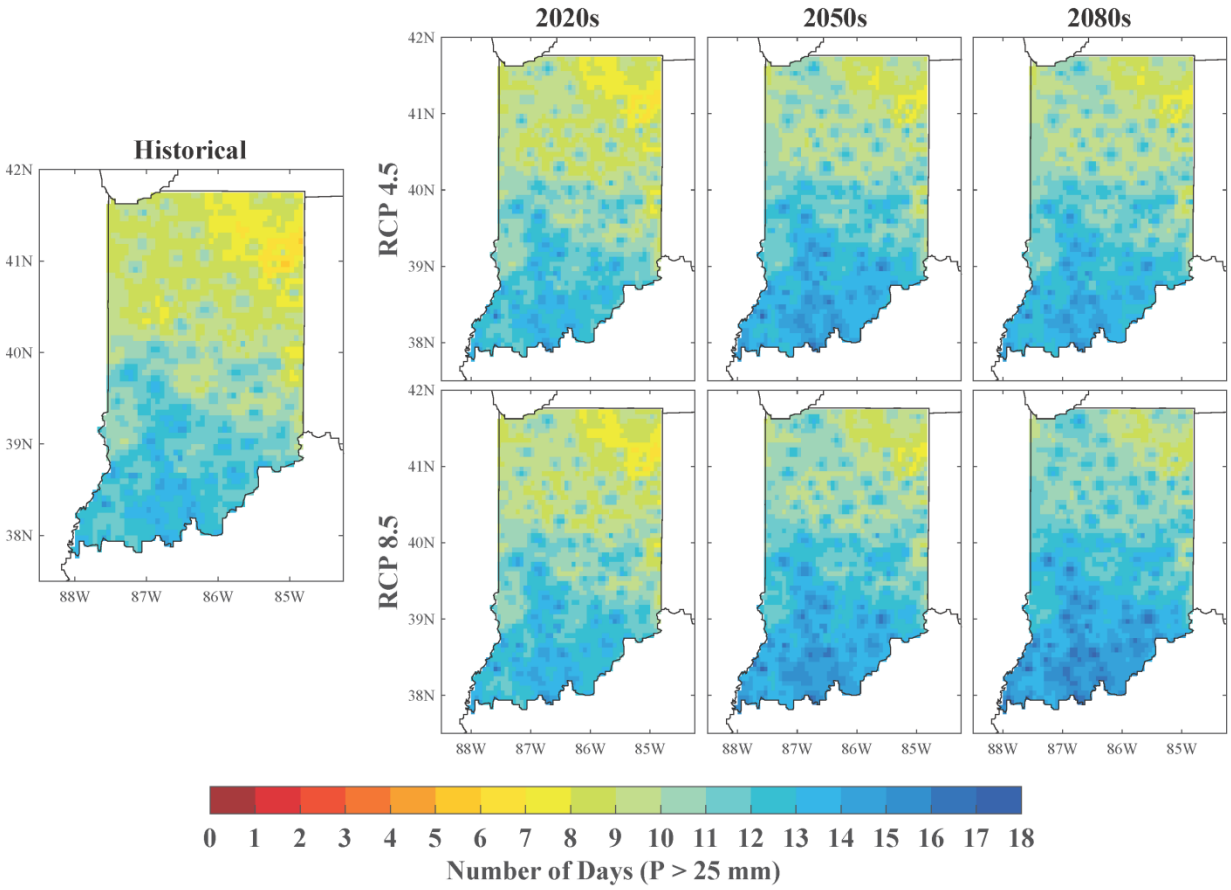


**Figure S8.** Ensemble average number of days with more than 25mm of precipitation. Seven panels: Historical (1915-2013) and 2020s, 2050s, 2080s for the RCP4.5 and RCP8.5 emissions scenarios. [Method: Type I, ensemble average of annual number days with more than 25 mm of P]

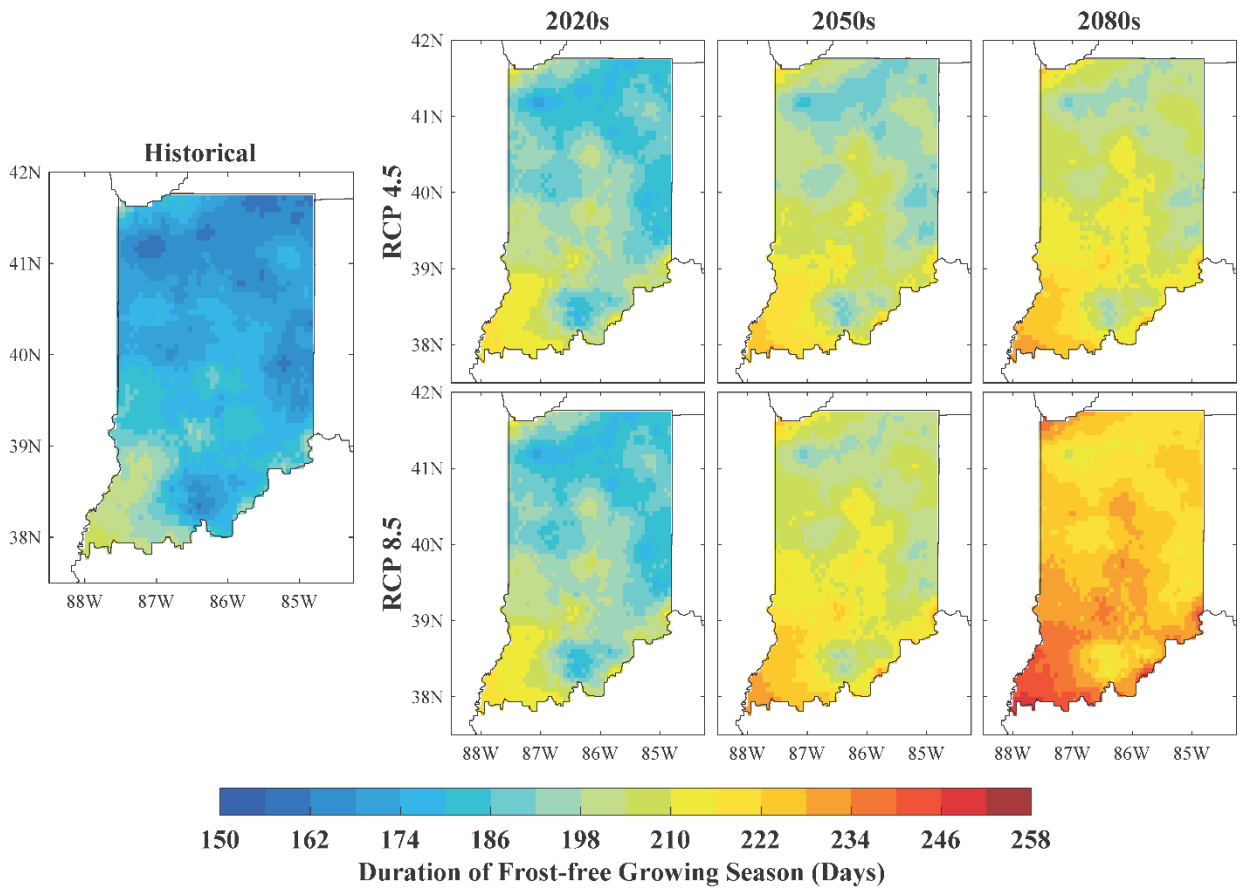


**Figure S9.** Ensemble average duration of frost-free growing season. Seven panels: Historical (1915-2013) and 2020s, 2050s, 2080s for the RCP4.5 and RCP8.5 emissions scenarios [Method: Type I, annual number of consecutive frost free days].

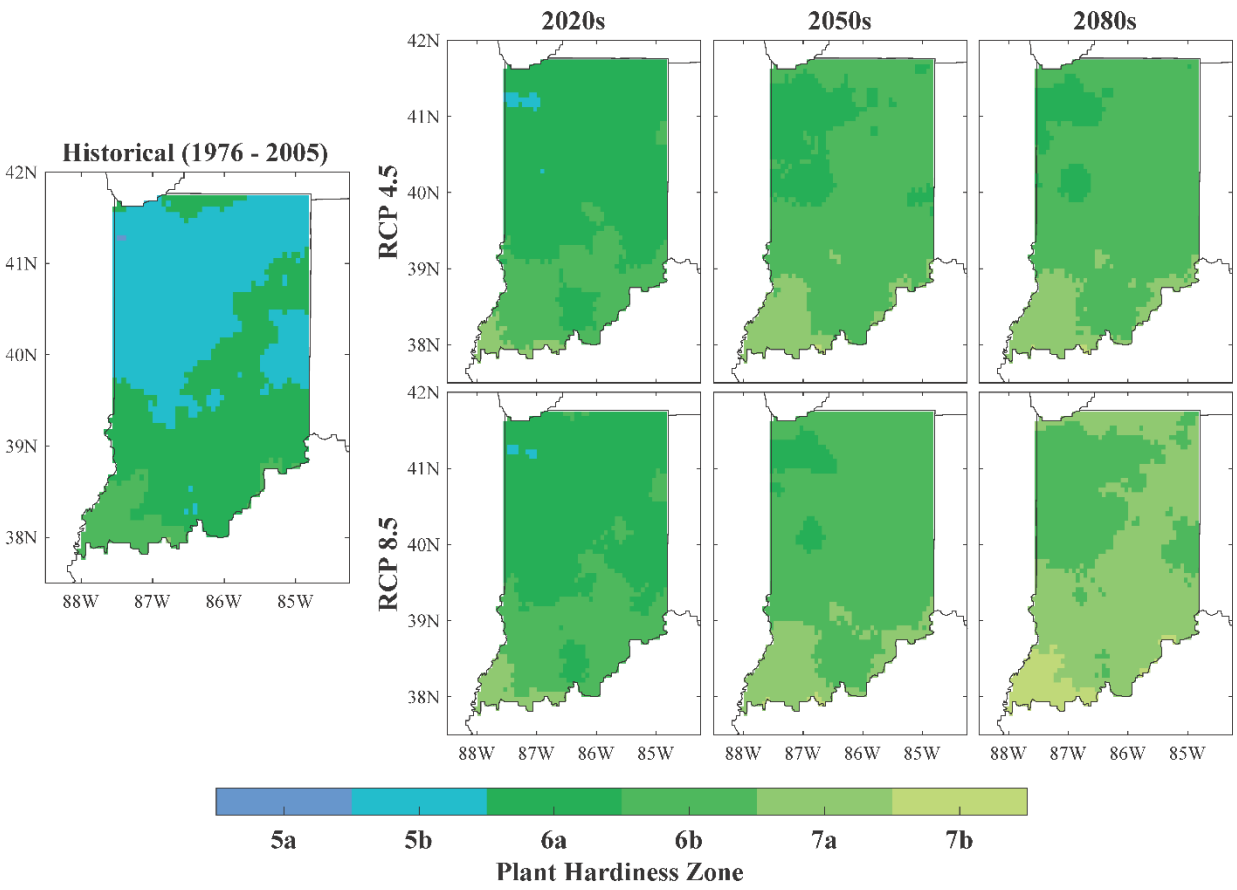


**Figure S10.** (seven panel) Maps of ensemble average USDA Plant Hardiness Zones. Seven panels: Historical (1976-2005) and 2020s, 2050s, 2080s for the RCP4.5 and RCP8.5 emissions scenarios [Method: Type I, plant hardiness zones]

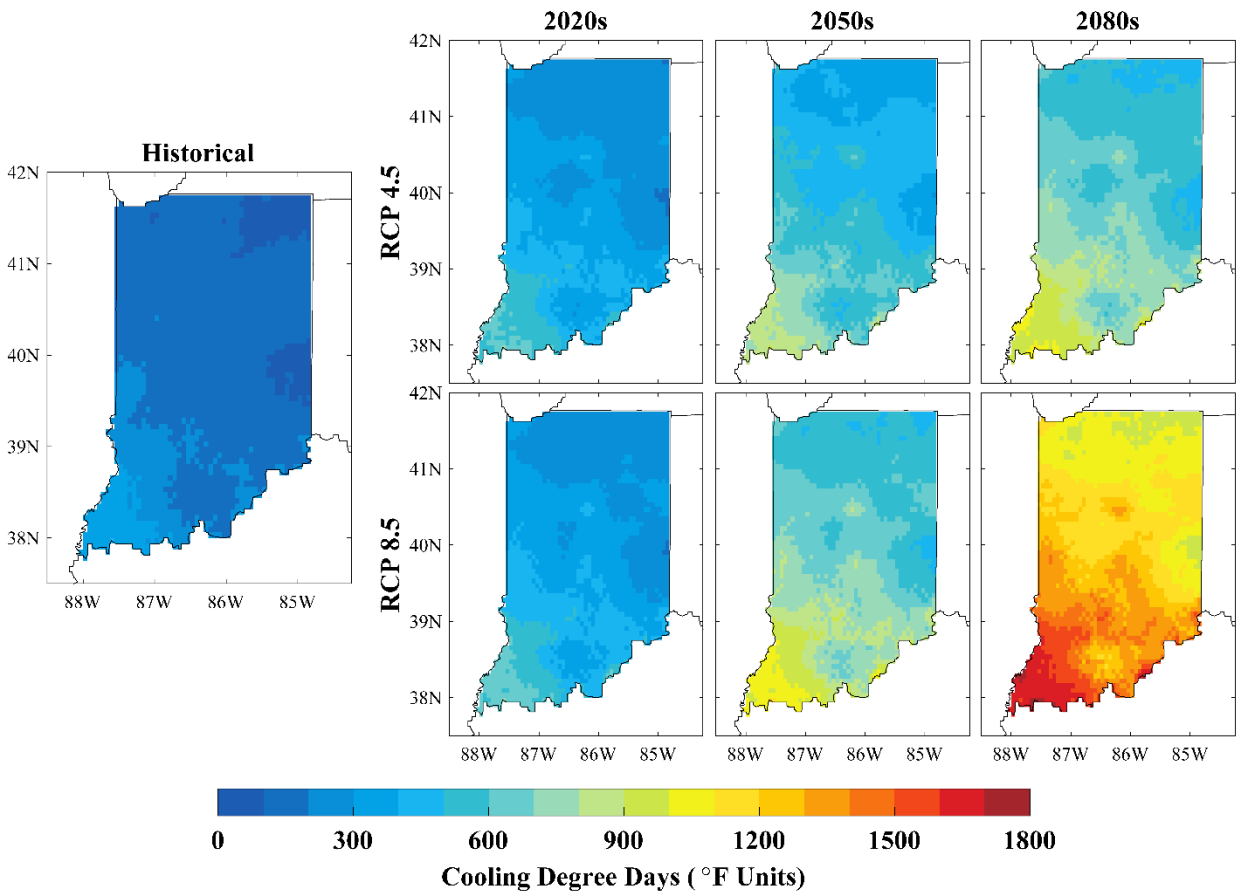


**Figure S11**. Ensemble-average, long-term mean annual total cooling degree days (°F units relative to 75 °F). Seven panels: Historical (1915-2013) and 2020s, 2050s, 2080s for the RCP4.5 and RCP8.5 emissions scenarios. [Method: Type I, ensemble average of annual total cooling degree days]

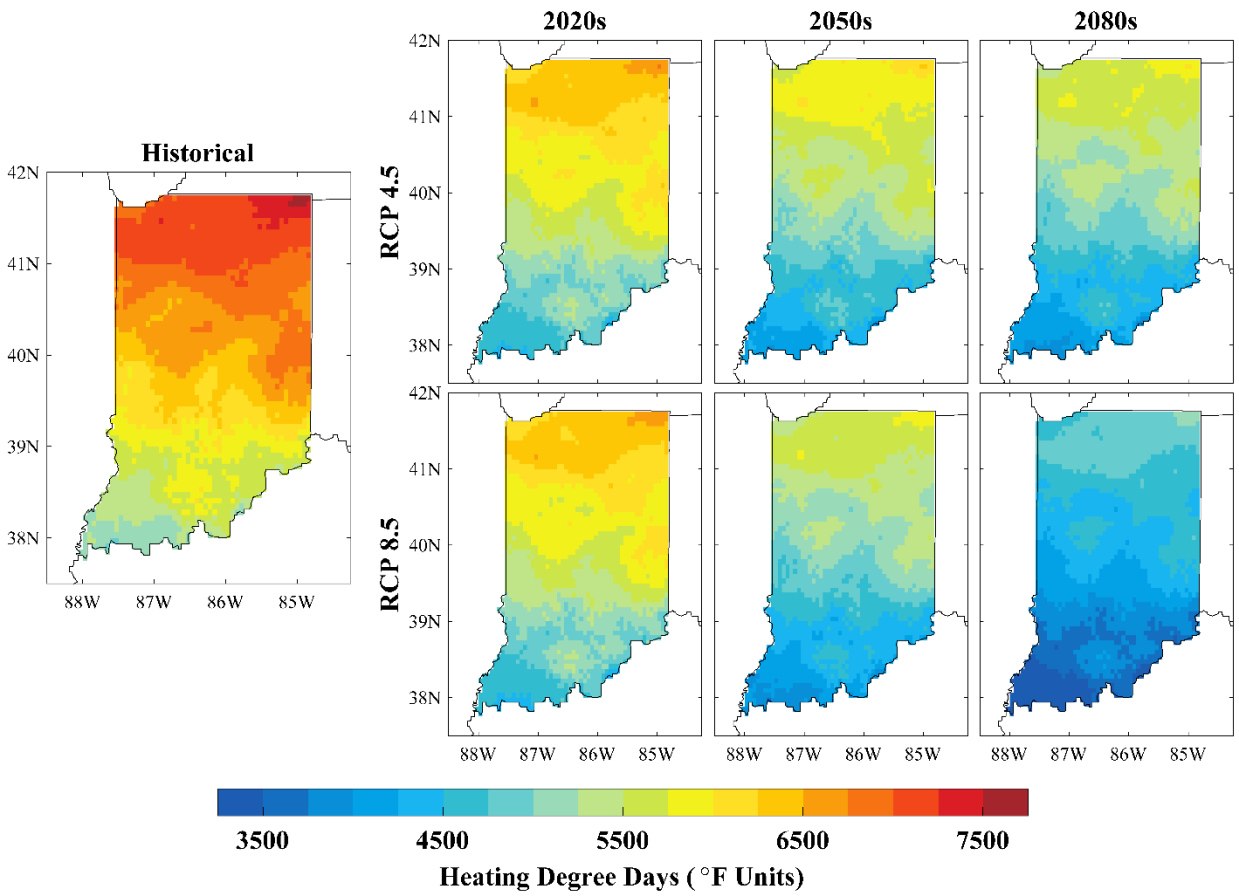


**Figure S12.** Ensemble-average, long-term mean annual total heating degree days (°F units relative to 68 °F). Seven panels: Historical (1915-2013) and 2020s, 2050s, 2080s for the RCP4.5 and RCP8.5 emissions scenarios**.** [Method: Type I, ensemble average of annual total heating degree days]

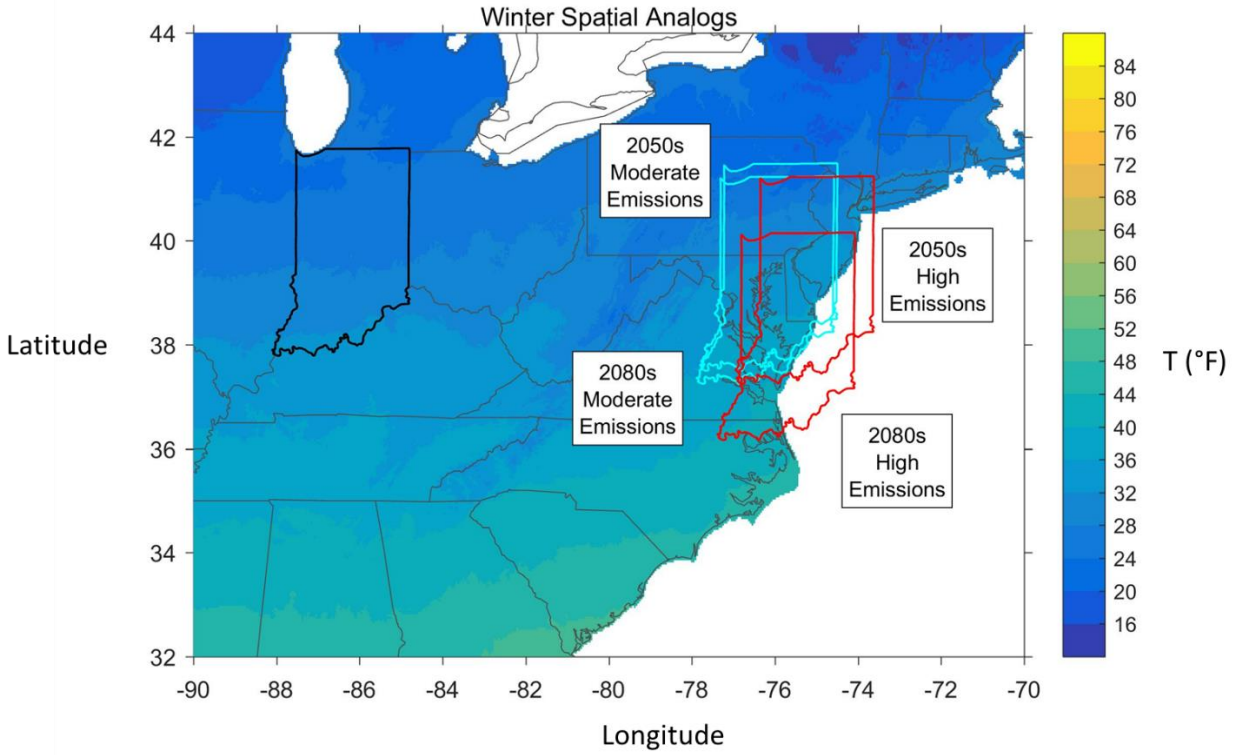


**Figure S13.** Spatial analogues for IN based on the best fit for IN's future T and P projections in winter. Historical analogues are based on PRISM long-term average monthly T and P data (Daly et al. 2008).

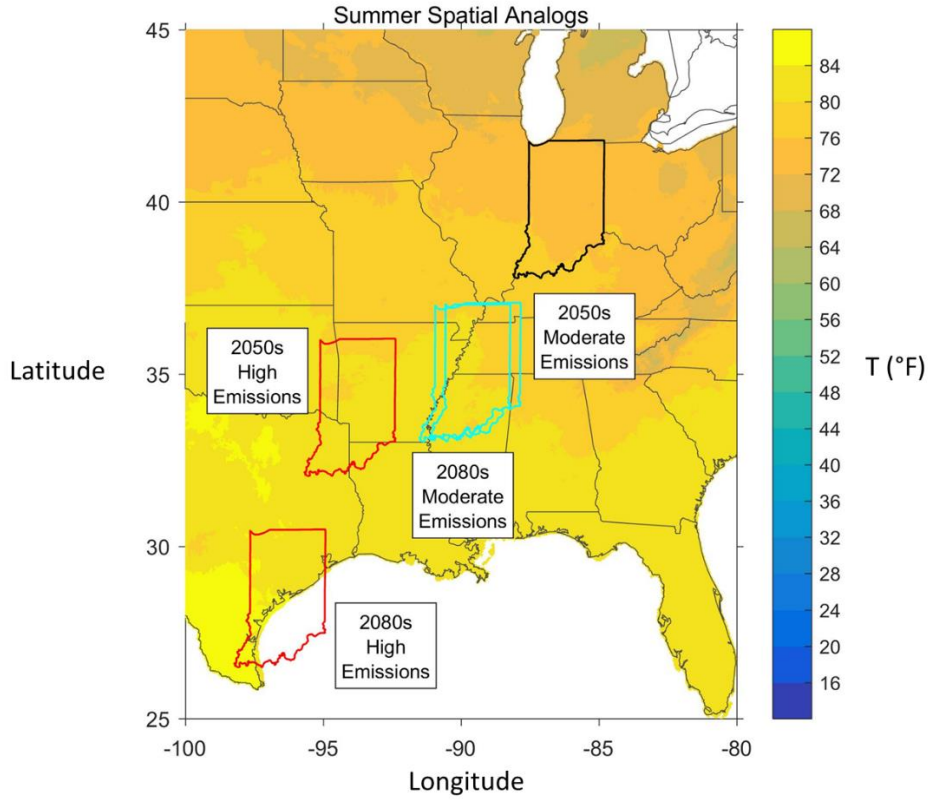


**Figure S14.** Spatial analogues for IN based on the best fit for IN's future T and P projections in summer. Historical analogues are based on PRISM long-term average monthly T and P data (Daly et al. 2008).